Cukurova University
Journal of
Natural & Applied Sciences

Original Paper

New achievements of remote sensing at the stage of geological exploration research: from satellite images to the determination of the ore body

Akram Bayramovich Goipov[1,2], Mehmet Ali Akgül[3], Suphi Ural[3], Shokir Islomovich Akhmadov[1]

[1]Department of Digital Mapping, Institute of Mineral Resources, Tashkent, Uzbekistan
[2]Faculty of Geology of Mineral Deposits, University of Geological Sciences, Tashkent, Uzbekistan
[3]Department of Mining Engineering, Cukurova University, 01330 Adana, Turkey

ORCID IDs of the authors: A.B.G. 0000-0003-1720-2998; M.A.A. 0000-0002-5517-9576; S.U. 0000-0003-4865-011X; S.I.A. 0000-0002-8983-9763.

Cite this article as: Goipov A. B., Akgül, M. A., Ural, S., Akhmadov, S. I. (2023). New achievements of remote sensing at the stage of geological exploration research: from satellite images to the determination of the ore body, Cukurova University Journal of Natural & Applied Sciences 2(1): 27-36.

Abstract

As a result of work using the ratio of different bands and combinations of Landsat 7 and Landsat 8 multispectral satellite images, a new combination was created, which made it possible to map mineralization zones for known deposits and identified new potentially promising mineralized zones as continuations of ore zones. The results of remote studies are provided as contours of predictive positions, which are identified by spectral anomalies in the short-wave infrared (SWIR) ranges. These anomalies are confirmed by traditional methods of geological research in the field. The samples obtained along the exploration routes showed a high content of gold and associated minerals. By processing the iron index of multispectral space images, we obtained correspondence to the zones of hydrothermal changes. The ratio of increase in mineralization content is related to the distribution density of spectral halos. With remote sensing methods, field verification work and structural studies were carried out in parallel, as a result of which the impact of Quaternary tectogenesis was established, which led to a change in ore bodies to a lenticular shape.

Keywords: Kuljuktau, Remote sensing, Landsat.

1. Introduction

The global experience of industrialized nations in satellite technology over the past two decades has demonstrated that the use of remote sensing materials in geology is a dependable and successful strategy. In remote sensing operations, automated methods of processing satellite images recorded in multispectral range using diverse sensors play a crucial role.

For remote identification of mineral formations in the relief from a wide variety of electromagnetic spectrum spectra, 0.4-2.5 μm wavelength is typically employed. SWIR wavelengths between 2.0 and 2.5 μm are of particular importance. Particularly in this epoch, the principal spectra of hydroxides, sulfates, and carbonates are recorded, which are indicative of various rocks and secondary hydro-thermal modifications. Zones of silicification, sulfidization, argillitization, propylitization, etc. are detected at various spectral intervals in thermal and other infrared bands.

The primary gold deposits in the Central Kyzylkum region are of the hydrothermal genetic type [1]; therefore, it is appropriate to apply satellite image processing techniques with a variety of methodologies and indices. VNIR (visible and near infrared) and SWIR

Address for Correspondence:
Mehmet Ali Akgül, e-mail: mali.akgul@dsi.gov.tr

Received: Jan 11, 2023
Accepted: Mar 10, 2023

(shortwave infrared) bands are utilized to map mineral indices and secondary hydrothermal alteration with remote sensing techniques. Landsat photos have been utilized for decades in numerous sectors of Earth science, including the hunt for various metal minerals. Iron oxide was identified for the first time using Landsat MSS Data [2] and new Landsat 8/OLI pictures, which are characterized by great productivity in the discovery of iron oxides even in densely vegetated regions [3].

In this study, we used the results of using the principle component approach and Crosta technology to determine the zone of clay mineral and iron oxide accumulations using Landsat 7 and Landsat 8 multispectral satellite pictures. This study is an experimental and methodological investigation of the use of Landsat 7 and 8 image processing data for mapping mineral, secondary, and hydrothermal alteration zones. Listed below are the accomplishments of a few researchers in the field of remote sensing for tackling diverse geological issues.

The VNIR and SWIR bands of Landsat 5 TM satellite photos were utilized to map lithological changes [4]. The application Landsat 7 is used to map geological heterogeneity [5-8]. The ability of Landsat-7 bands to detect iron oxide [9] and hydroxide minerals using 3/1 ratio imaging and mapping of hydroxyl bearing minerals and carbonates using satellite images with 5/7 band ratio, respectively [10-13] and mapping of hydrothermal alteration [14, 15]. Landsat-7 bands are capable of detecting iron oxide [9] and hydroxide minerals with 3/1 ratio imaging, as well as mapping hydroxyl bearing minerals and carbonates with 5/7 band ratio satellite imagery [10-13] and hydrothermal alteration mapping [14, 15], respectively.

The objective of this project is to map the geological and structural aspects of the Kuljuktau mountains in the Central Kyzylkum region, as well as to detect mineralization zones, using remote sensing techniques. It is seen that it is appropriate to use remote sensing studies, which are both faster and more economical than terrestrial studies, in studies that spread over such a wide area.

2. Material Method

2.1. Study area

The Taushan gold deposit and other deposits and ore occurrences in the Kuljuktau mountains are the focus of this study (Figure 1). The Kuljuktau Mountains are a modest sublatitudinal ridge with heights between 400 and 785 meters. The ridge is between 8 and 12 km wide and 84 km long.

The region's climate is strongly continental, as is typical of the desert. Summer is dry and scorching, while winter is freezing and snowless. The highest temperature in July (according to the Dzhengeldinskaya meteorological station) is +45 - 47, and the lowest is -20 - 24. (in January). The annual precipitation does not exceed 90-100 mm, and 90% of precipitation falls between December and May. There are consistent northern breezes throughout the year, occasionally accompanied by dust storms. The vegetation is characterized by the development of herbaceous forms that are resistant to drought. No surface watercourses exist in the work area.

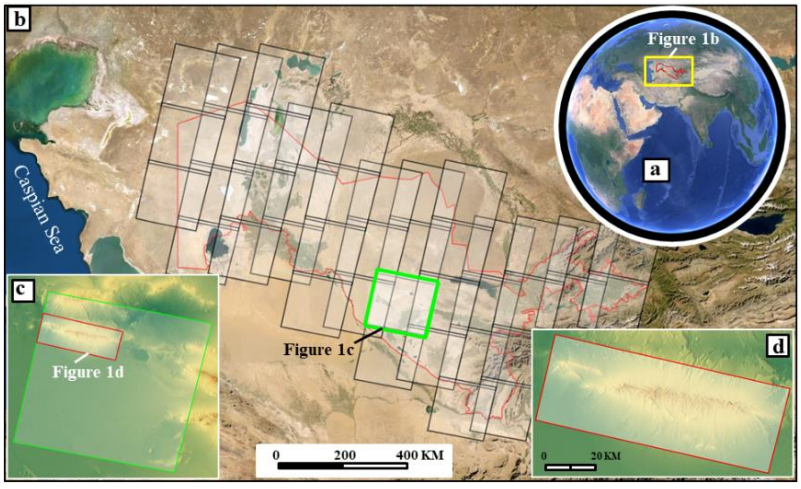

Figure 1. Overview map of the area of study: a) position of the territory of Uzbekistan on a world map; b) space survey of Central Asia with Landsat series satellite imagery of the territory of Uzbekistan; c) location of the study region in one Landsat series imagery; and d) digital terrain model of the study area (SRTM)

Numerous researchers were engaged in the geological study of the Kuljuktau mountains and adjacent territories. Geological surveys of scale 1:1000 000 - 1:200 000, as a result of which the lithological and stratigraphic strata of the Paleozoic and Meso-Cenozoic stages were identified, were conducted in the area from 1927 to 1963 years. From 1963 to 1972, a 1:50 000 – scale state geological survey was conducted in the Kuljuktau Mountains [16].

According to this, the geological structure of the area involves sedimentary-metamorphic and eruptive rocks of Paleozoic age, composing mountain uplands and forming a folded basement, deposits of Cretaceous, Paleogene, Neogene systems, developed, mainly on foothill plains and related to the cover [17].

In the Paleozoic geosynclinal complex includes volcanogenic-terrigenous, partly carbonate formations of Ordovician, thick carbonate formation of Silurian, Devonian, Lower Carboniferous, volcanogenic-terrigenous and molasse formations of Middle and Upper Carboniferous. The Cretaceous (except for the Aptian, Middle Upper Albian), Paleogene, and Miocene sections are represented by marine facies; rocks of the Aptian, Middle Upper Albian, and Quaternary suborders are present in continental facies [18].

The Kuljuktau Mountains in the modern tectonic structure are an Alpine uplift of sublatitudinal strike (Figure 2), composed of rocks of Paleozoic folded basement in the core and sediments of Meso-Cenozoic sedimentary cover in the wings. Intensely dislocated sedimentary and magmatic complexes corresponding to the geosyncline stage of the region [18] represent the folded basement. The cover is formed by relatively thin (up to 1200 m) sediments, which emerged during the platform stage of development [17, 19, 20].

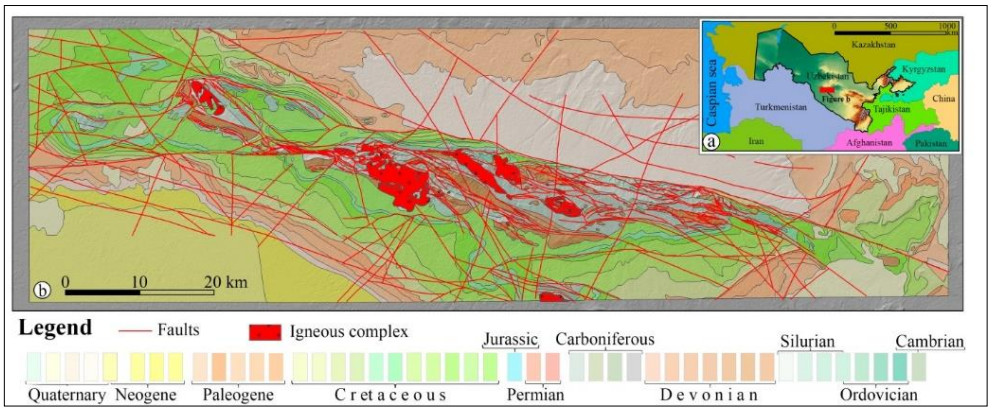

Figure 2. Geological map of the Kuljuktau mountains

Based on the nature of the stratigraphic section [18], the age of folding [16], and the specificity of magmatism [21], the Paleozoic formations of the Kuljuktau mountains belong to the Zarafshan-Alay structure formation zone [19, 22], which is located in the southern portion of the South Tien Shan geosyncline system and was deposited in the Lower Paleozoic on the Precambrian basement [17].

Magmatic formations account for around 15% of the Kuljuktau Mountains' total area. Quantitatively speaking, granitoid and gabbroic intrusive rocks predominate among them [18, 21]. 548 km^2 comprise the outcrop of Paleozoic rocks in the **Kuljuktau** Mountains. The amount of ore per 100 square kilometers is 39 items. Taushanskoe, Adylsayskoe, Yuzhno-Sultanbibiyskoe, Aktostinskoe, and Yangikazganskoe are the five most important ore deposits in this region.

According to the plan of metallogenic zoning of Western Uzbekistan [23], the Kulzhuktau mountain range is a part of the Zarafshan-Gissar ore belt – W, Sn, and Cu (As, Mo, Sb, Pb, Zn). Later [24, 25] it was demonstrated that this belt should be categorized as gold-tungsten-tin-antimony-mercury, with distinct ore zones, nodes, and clusters of ore fields.

To map mineral changes using remote sensing data to detect new locations and mineralization zones, a map of geochemical anomalies was examined (Figure 3). According to the plan of metallogenic zoning of Western Uzbekistan [23], the Kuljuktau mountain range is a part of the Zarafshan Gissar ore belt - W, Sn, and Cu (As, Mo, Sb, Pb, Zn). Additional [24, 25] evidence suggests that this belt should be considered a gold-wolfram-tin-antimony-mercury belt, which has a variety of ore zones, knots, and ore field clusters

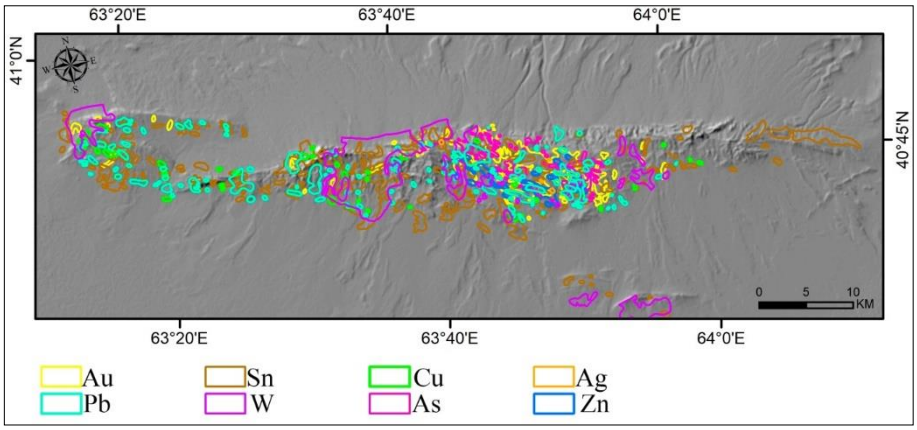

Figure 3. Halos of geochemical field anomalies (according to the generalized data of previous works)

In the Kuljuktau mountains, a substantial number of deposits, ore occurrences, and mineralization points, the majority of which are endogenous of different genetic kinds, were discovered in the development fields of pre-Carboniferous carbonate strata [1].

2.2. Material

Utilizing multitemporal satellite images Landsat 7 with an installed sensor ETM + (The Enhanced Thematic Mapper Plus), Landsat 8 operational ground-based thermal imager OLI (The Operational Land Imager), and Landsat 8 operational groundbased thermal imager OLI (The Operational Land Imager), various methods and algorithms of methods for processing remote sensing materials were utilized in the performance of this work (Table 1).

Table 1. Landsat 7 and Landsat 8 satellite band specifications [26, 27]

Characteristics of Landsat 7 Bands			Landsat 8 Bands		
Band	Permission	Wavelength (μm)	Permission	Wavelength (μm)	Band
			30 m Coastal / Aerosol	0.435 – 0.451	Band-1
Band-1	30 m Blue	0.441 – 0.514	30 m Blue	0.452 - 0.512	Band-2
Band-2	30 m Green	0.519 – 0.601	30 m Green	0.533 - 0.590	Band-3
Band-3	30 m Red	0.631 – 0.692	30 m Red	0.636 - 0.673	Band-4
Band-4	30 m NIR	0.772 – 0.898	30 m NIR	0.851 - 0.879	Band-5
Band-5	30 m SWIR-1	1.547 – 1.749	30 m SWIR-1	1.566 – 1.651	Band-6
Band-6	60 m TIR-1	10.31 – 12.36	10 0 m TIR-1	10.60 – 11.1 9	Band-10
			10 0 m TIR-2	11.50 – 12.51	Band-11
Band 7	30 m SWIR- 2	2.064 – 2.345	30 m SWIR- 2	2.107 – 2.294	Band-7
Band-8	15 m Pan	0.515 – 0.896	15 m Pan	0.503 – 0.676	Band-8
			30 m Cirrus	1.363 – 1.384	Band-9

Several models and corrections are employed in the preliminary preparation of space pictures for spectral processing. When downloading Landsat 8 images from a public website, a notepad file (METADATA FILE) containing the survey area's metrological data is supplied. In the process of surveying a territory using a satellite sensor, the brightness values are distorted by the natural conditions of the provided region and the design of the satellite sensor. Radiometric calibration was done in the Radiometric calibration module of ENVI5.4 to restore the brightness value.

2.3. Method

Then, in order to reach the specified objectives, it is required to specify the water vapor parameters and execute the atmospheric correction in the ENVI 5.4 program using the MODTRAN environment settings as the standard parameters (water vapor content and near-surface temperature). The majority of the gold deposits in the Central Kyzylkum region are of the hydrothermal genetic type, thus the application of satellite image processing techniques employing a variety of methodologies and indices is acceptable.

Several methodologies and algorithms for remote sensing data processing utilizing multi-temporal satellite pictures Landsat 7 and 8 (Figures 4 and 5) were utilized during the research. The remote sensing geological surveys conducted in accordance with the idea of

sequential approach during the study of the subsoil: from the general to the particular, were able to expose the regional geological characteristics of the land and the structures manifested on it (Figures 4 and 5). For the identification of mineral components and minerals, band relations B5/B7 were utilized; for the identification of iron minerals B5/B4 and iron oxide B3/B1 were utilized.

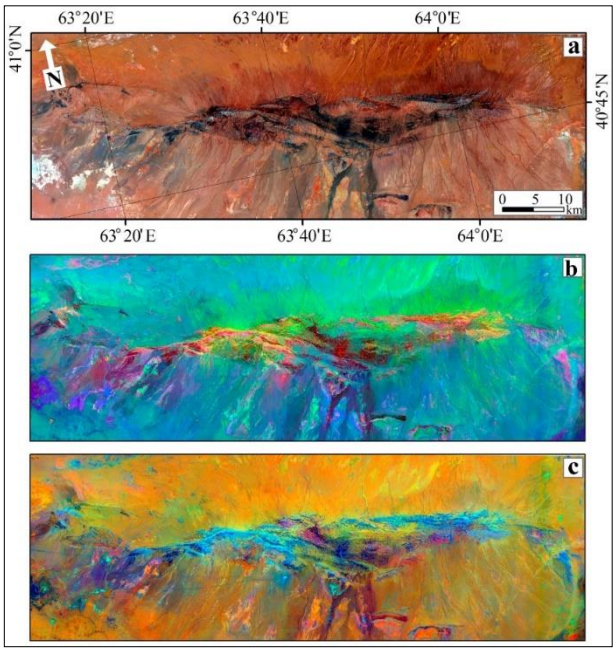

Figure 4. The outcomes of ratio bands processing applied to Landsat OLI satellite images: a) bands 5/3/2; b) bands 6/7, 6/4, 4/2; c) 5/7, 3/1, 4/3

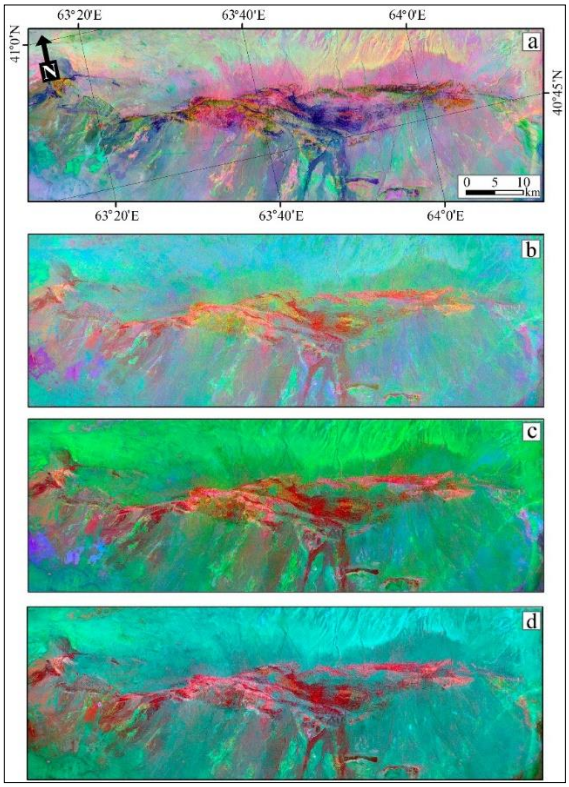

Figure 5. Outcomes of satellite image processing using Landsat ETM+ a) 7/5, 5/4, 3/1 (Gad & Kusky, 2006); b) 5/7, 3/1, 4/3 (Ciampalini & al., 2012); c) 5/3, 3/1, 7/5 (Achek and Aidouni, 2014)

3. Results and Analysis

The production of kaolinite and hydromica minerals in oxidation zones is a highly distinctive sign of mineralization. To detect kaolinite mineralization zones in this instance, the iron index and kaolinite index approaches must be utilized. Combinations of satellite image ratios are used to detect mineral components and minerals. For the detection of ferruginous minerals - B5/B4 and iron oxide - B3/B1 and kaolinitization, the Landsat 7 bands B5/B7 were used (Figure 6 and 7).

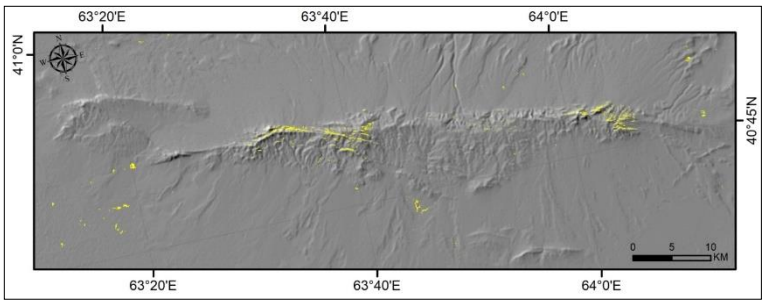

Figure 6. Iron oxide zones identified using the Hillshade effect and placed on a digital elevation model

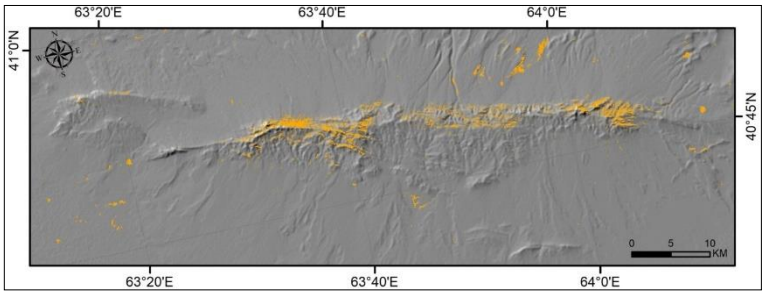

Figure 7. Kaolinitization zones identified and superimposed on a digital relief model utilizing the Hillshade effect

According to the results of satellite image processing, the primary sites of ore mineralization and mineralization zones coincide in many cases to the mapped zones of the iron index and kaolinization zones in the research region. As a consequence of study utilizing the ratio of different bands and a combination of multispectral band, a new combination was established, which made mineralized zone mapping possible (Figure 8).

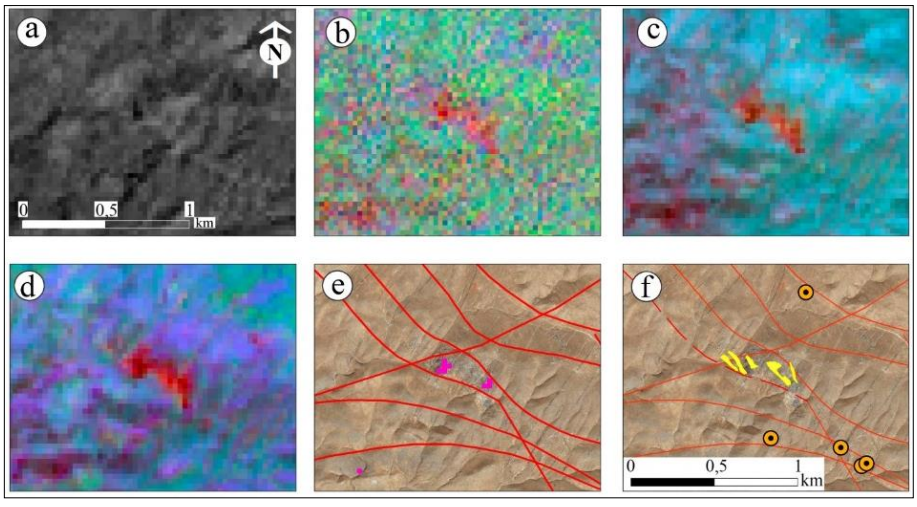

Figure 8. The outcomes of multispectral space image processing Landsat 7 and 8: a) flotband-2; b) LC-7; c) LC-8 6/7, 6/5, 6/4; d) LC-8 6/7, 4/2, 5/4; e) iron oxide; f) ore body and mineralization spots (according to [16])

The relationships between the spectral bands R=B7, G=B4, and B=B2 enabled the study of geological processes and the identification of types of soils, sands, and minerals exhibiting a vast array of colors and tones. Component mineral mixed with component hydrothermal b5/b7; b5/b4; b3/b1; b4/b3. Iron index was identified using false-color compositions, Band ratios, and main component analysis [9]. Using this method in prior research, we obtained valid data from another region of the Central Kyzylkum [29, 30].

When analyzing the middle portion of the Kuljuktau mountains, the application of the Landsat 7 and Landsat 8 band correlation method enabled the selection of the Taushan deposit (gold-quartz type) as a reference object. In order to map the hydrothermal alteration zone, the Band ratio of Landsat multispectral space pictures was processed for the iron index (Figure 9).

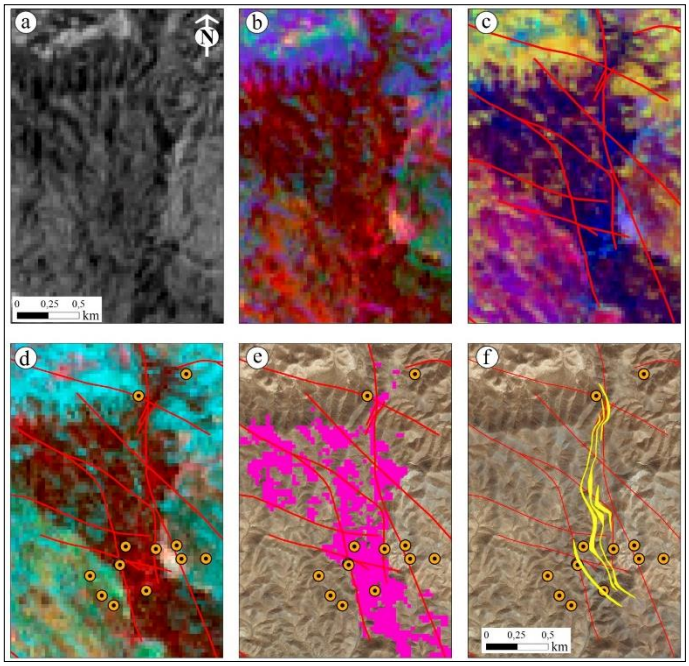

Figure 9. Outcomes of Landsat 7 and 8 multispectral space image processing of the Taushan deposit reference object (assembled by Goipov): a) floatband-2; b)LC-8 6/7, 4/2, 5/4; c) LC-8 7/5, 5/4, 6/7; d) LC-8 6/7, 6/5, 6/4; e) iron oxide; f) ore body and mineralization points (based on [16])

Figure 9a demonstrates that the single-Band space image is non informative, and that mapping the zones of secondary and mineral alterations before to the delineation of the ore body is possible utilizing processing techniques established by foreign researchers and algorithms created by us. Using this method to gather data for the Taushan deposit area, it is possible to recommend these data for iron index mapping of the entire Kuljuktau mountain range (Figure 9).

Figures 9e and 9f demonstrate that, in many instances, the primary ore mineralization and mineralization zones correlate to the mapped iron index zones. Middle Carboniferous terrigenous sediments make up the Taushan deposit (siltstones, sandstones, shale). The rocks are sliced by alkaline lamprophyre and diabase porphyrite dikes. Fracture tectonics is illustrated by sublatitudinal faults that dip steeply and strike to the northwest. According to geological data, the arrangement of ore-bearing zones in the deposit is determined by northwest faults. Two tectonic mineralized zones trending northwest have been identified (Figure 9f). Northwestrending faults control the placement of the ore-bearing zones of the deposit. Two tectonic mineralized zones with a northwest orientation have been identified. One of them (central) is 2 kilometers long and up to 200 meters thick and holds the majority of the deposit's ore.

According to the material composition, the gold-quartz ore formations correspond to the low-sulfide type. Gold is the sole commercially valuable component. At the deposit, the oxidation zone, which reaches to a depth of 60-70 meters, is examined primarily. In the oxidation zone, native gold is present in the intergrain space, in cracks and voids caused by leached minerals, generating irregularly shaped, wire-like, and lumpy xenomorphic precipitates. The ore minerals iron hydroxides, covelline, and chalcosine represent. Non-ore: quartz, mica, feldspars, clay minerals, carbonates, carbonaceous materials, gypsum, talc, chlorite, epidote [1]. In 1997, the State Reserve Committee of the Republic of Uzbekistan approved explored reserves.

Prior to this, only seven commercial ore occurrences associated with metasomatically altered rocks and variously oriented thin quartz veins had been investigated. These zones have been confirmed using spectral Band correlations RGB, B7, B4, and B2, and new previously unknown mineralized zones have been found. After satellite image processing, field verification was conducted to confirm the identified zones (Figure 10).

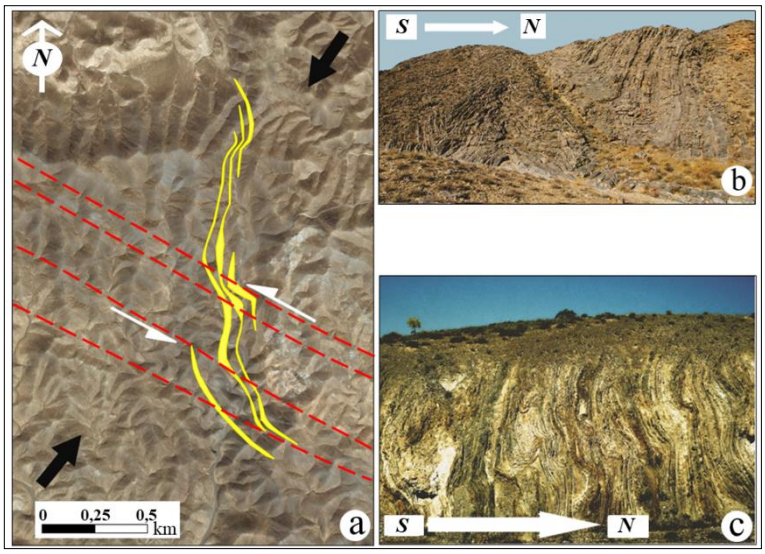

Figure 10. Structural examination of the Taushan gold deposit parallel sublatitudinally strike-slip fault zone in compression zones formed following ore formation: a) ore body of the Taushan deposit on the super high resolution satellite image; b) folding and fracture deformation in the sediments of the lower portion of the Sultanbinsk formation Lower-Middle Devonian northwest of the Uchkuduk well; c) Lower portion of the Arapkazgan formation Lower-Upper Devonian, outcrops on the right side of the Arapkazgan formation

At the prospecting and assessment stage of ore zones, it is vital to determine the spatial position of ore zones in consideration of the formation of tectonic, deformational states preceding and following ore formation. Compression along the NE-SW to NNE direction generated pre-ore deformation, which resulted in the creation of fracture zones from NW to sublatitudinal orientations, as well as folds, fractures, and associated shears (north-northeast right-lateral and east-northeast left-lateral). During the time of left-lateral compressive deformation, which was apparently connected with the major collision/accretion phase of the belt, these zones formed. The sublatitudinal structural orientation may mirror, in part, the sublatitudinal orientation of the sutural zone.

The gold mineralization was developed during the same accretionary stage, but was governed by a subsequent phase of right-lateral compression (NNW-SSE) with large strike-slip displacements along strike. This may have occurred as a result of the termination of subduction, when fluids were released as a result of temperature equilibrium in subplit/accretionary rocks associated with deep late metamorphism. The slight deformation of the veins and the tight association of the mineralization with the lamirophyrobae dikes, which may serve as an excellent indication for prospecting, indicate this.

At the Taushan deposit, the transverse structure is represented rather plainly; it consists of an extensive north-northwest trending fault with subparallel folding (Figure 10a). It contains gold ore bodies and pre-ore dikes. In the Adylsay ore occurrence, which is located southeast of the Taushan deposit, the cross-sectional fault is less obvious, its extent and thickness are less, and it is less extensive. Its entire transverse structure is likewise rich in late dykes and gold mineralization.

4. Conclusions

The results of processing satellite images using various techniques revealed a high degree of congruence in the occurrence of the ore body, which was manifested in the hydrothermal anomalies and zones of secondary change registered in the infrared range; that is, the invisible spectral range reveals geological-lithological and mineralogical heterogeneities, as well as other aspects of the phenomenon or process under investigation.

False colors, as well as the ratio of Landsat 7 and Landsat 8 bands by techniques of iron index and iron oxide, were able to expose the geographical position of the reference ore zone on the land of the Kuljuktau mountains, leading in the identification of new gold-promising mineralization zones. Throughout the course of field verification work, samples were collected from anomalous zones;

laboratory examination revealed a high concentration of valuable components and their satellites. Geological prospecting is advised in the identified prospective regions.

References

[1] Golovanov, I.M. (2001). Ore deposits of Uzbekistan. - T.: HIDROINGEO. 660 p.

[2] Segal, D. (1982). Theoretical Basis for Differentiation of Ferric-Iron Bearing Minerals, Using Landsat MSS Data. Proceedings of Symposium for Remote Sensing of Environment, 2nd Thematic Conference on Remote Sensing for Exploratory Geology, Fort Worth, TX: pp. 949-951.

[3] Ducart, D.F., Silva, A.M., Toledo, C.L.B., Assis, L.M. (2016). Mapping iron oxides with Landsat 8/OLI and EO-1/Hyperion imagery from the Serra Norte iron deposits in the Carajás Mineral Province, Brazil. Brazilian Journal of Geology. 46(3): 331-349...

[4] Gad, S., Kusky, T. (2006). Lithological Mapping in the Eastern Desert of Egypt, the Barramiya Area, using Landsat Thematic Mapper (TM). Journal of African Earth Sciences. 44: 196-202.

[5] Ciampalini, A., Garfagnoli, F., Del Ventisette, C., Moretti, S. (2013). Potential Use of Remote Sensing Techniques for Exploration of Iron Deposits in Western Sahara and Southwest of Algeria. Natural Resources Research. 22. doi:10.1007/s11053-013-9209-5.

[6] Salem, SM, El Gammal, EA. (2015). Iron ore prospection East Aswan, Egypt, using remote sensing techniques, Egypt. J. Remote Sensing Space Sci. doi:10.1016/j.ejrs.2015.04.003

[7] Vural, A., Corumluoglu, O., Asri, I. (2016). Exploring Gördes Zeolite Sites by Feature Oriented Principle Component Analysis of LANDSAT Images. Caspian Journal of Environmental Sciences. 14(4): 285-298.

[8] Amri, K., Rabai, G., Benbakhti, I.M., Khennouche, N. (2017). Mapping geology in Djelfa District (Saharan Atlas, Algeria), using Landsat 7 ETM+ data: an alternative method to discern lithology and structural elements. Arabian Journal of Geosciences. 10. doi:10.1007/s12517-017-2883-6.

[9] Ciampalini, A., Garfagnoli, F., Antonielli, B., Moretti, S., Righini, G. (2012). Remote sensing techniques using Landsat ETM+ applied to the detection of iron ore depositsin Western Africa. Arabian Journal of Geosciences. doi:10.1007/s12517-012-0725-0

[10] Ramadan, T.M., Kontny, A. (2004). Mineralogical and structural characterization of alteration zones detected by orbital remote sensing at Shalatein District area, SE Desert, Egypt. Journal of African Earth Sciences. 40: 89-99.

[11] Al-Rawashdeh, S., Saleh, B., Hamzah, M. (2006). The Use of Remote Sensing Technology in Geological Investigation and Mineral Detection in El Azraq-Jordan. Cybergeo: European Journal of Geography, Systèmes, Modélisation, Géostatistiques. 358: 1-21.

[12] Dogan, H. (2009). Mineral composite assessment of Kelkit River Basin in Turkey by means of remote sensing. Journal of Earth System Science. 118: 701-710. doi:10.1007/s12040-009-0059-9.

[13] Shalaby, M.H., Bishta, A.Z., Roz, M.E., Zalaky, M.A. (2010). Integration of geologic and remote sensing studies for the discovery of uranium mineralization in some granite plutons, Eastern Desert, Egypt. Journal of King Abdulaziz University, Earth Sciences. 21: 1–25.

[14] Pour, A.B., Hashim, M. (2015). Hydrothermal alteration mapping from Landsat-8 data, Sar Cheshmeh copper mining district, southeastern Islamic Republic of Iran. Journal of Taibah University for Science. 9: 155-166.

[15] El Atillah, A., El Morjani, Z., Souhassou, M. (2019). Use of the Sentinel-2A Multispectral Image for Litho-Structural and Alteration Mapping in Al Glo'a Map Sheet (1/50,000) (Bou Azzer–El Graara Inlier, Central Anti-Atlas, Morocco) Artificial Satellites. 54(3): 73-96. doi:10.2478/arsa-2019-0007.

[16] Aisanov, Y.B., Egorov, A.I. (1978). Geological structure and main features of mineralization of the Paleozoic formations of the Kuldzhuktau mountains. - Tashkent: Fan, 120 p.

[17] Mirkamalov, R.Kh., Chirikin, V.V., Divaev, F.K. (2019). Geodynamic reconstructions of the orogenic belt of the Western Tien Shan and forecasting of endogenous deposits in the basement rocks (guidelines). T.: SE Institute of Mineral Resources - 162 p.

[18] Shayakubov, T.S., Dalimov, T.N. (1998). Geology and Minerals of the Republic of Uzbekistan, Tashkent University, Tashkent. 724 pp.

[19] Biske, Y.S. (1996). Paleozoic structure and history of the Southern Tien Shan. - SPb., 192 p.

[20] Burtman, V.S. (2006). Tien Shan and High Asia Tien Shan and High Asia Tectonics and geodynamics in the Palaeozoic. Moscow. 214p.

[21] Konopelko, D.L. (2020). Paleozoic granitoid magmatism of the western Tien Shan. - SPb., 196 p.

[22] Bukharin, A.K., Maslennikova, I.A., Pyatkov, A.K. (1985). Pre-Mesozoic structural-formational zones of Western Uzbekistan. - Tashkent: Fan, 152 p.

[23] Khamrabaev, I.Kh. (1958). Magmatism and postmagmatic processes in Western Uzbekistan. Academy of Sciences of the Uzbek SSR, Tashkent.

[24] Khamrabaev, I.Kh. (1969). Petrological and geochemical criteria for ore content of magmatic complexes (on the example of Uzbekistan) // Tashkent: Fan. 210 p.

[25] Garkovets, V.G., Mushkin, I.V., Titova, A.P. et al. (1979). The main features of metallogeny in Uzbekistan. - Tashkent: Fan, 272 p.

[26] NASA. (1999). “Landsat 7 Science Data User's Handbook.” http://ltpwww.gsfc.nasa.gov/IAS/ handbook/handbook_toc.html.

[27] USGS. (2016). LANDSAT 8 (L8) Data Users Handbook. Department of the Interior US Geological Survey, LSDS-1574 Version 2.0, page:98.

[28] Achek, H., Aidouni, N. (2014). Essai de cartographie géologique par la télédétection optique de la région Hank (Sud-Ouest Algérien).

[29] Goipov, A.B., Akhmadov, Sh.I., Movlanov, J.J. (2020a). Study of mineralized zones of the Bukantau mountains using satellite images in the short-wave infrared range. Mining Journal of Kazakhstan. 8: 10-14.

[30] Goipov, A.B., Khasanov, N.R., Akhmadov, Sh.I. (2020b). Study of the mineralized zones of the Bukantau mountains on space images in the short-wave infrared range. Journal of Critical Reviews. 7(6): 2070-2074. doi:10.31838/jcr.07.06.322.